International Journal of Refractory Metals & Hard Materials 81 (2019) 119–126

Contents lists available at ScienceDirect

International Journal of Refractory Metals & Hard Materials

journal homepage: www.elsevier.com/locate/IJRMHM

Reactive spark plasma sintering of TiB_2–SiC–TiN novel composite

Mehdi Shahedi Asl[a,*], Seyed Ali Delbari[a], Farzad Shayesteh[a], Zohre Ahmadi[a], Amir Motallebzadeh[b]

[a] Department of Mechanical Engineering, University of Mohaghegh Ardabili, Ardabil, Iran
[b] Koc University Surface Science and Technology Center, Istanbul, Turkey

ARTICLE INFO

Keywords:
SPS
Microstructure
TiB_2
SiC
TiN
BN nano-platelets

ABSTRACT

The effects of adding SiC as a reinforcement and TiN as an additive on TiB_2-based composites fabricated by the spark plasma sintering (SPS) technique were investigated. SPS was implemented at the sintering conditions of 1900 °C temperature, 7 min holding time and 40 MPa pressure. Adding these two secondary phases had noticeable effects on the microstructure of TiB_2-based composites. A relative densities of 99.9% was obtained for TiB_2–SiC–TiN composite. Detection of in-situ formed phases and investigation on them were done using SEM, XRD, EDS and thermodynamic assessment. These evaluations proved the formation of in-situ phases of TiC, BN nano-platelets, TiSi and B_4C in the TiB_2-based composite codoped with SiC and TiN. Formation of these in-situ phases had fascinating effects on the sinterability and ultimate microstructure of titanium diboride.

1. Introduction

Over recent years, design and fabrication of advanced materials which are stable at high temperatures have been attracted lots of consideration among researchers. Ceramic materials including carbides, nitrides, beryllides, borides and silicides, due to their remarkable hardness and presentation of good properties at harsh thermal conditions, are the best candidates for high-tech structural applications. However, thanks to poor mechanical properties, the use of monolithic ceramics, even the fully dense ones, is limited in practical cases. Adding secondary phases, namely production of ceramic matrix composites (CMCs), offer many noticeable advantages such as better fracture toughness in comparison with unreinforced ceramics [1–10]. Moreover, recent research works have shown that the formation of in-situ phases during reactive sintering methods exhibits additional benefits compared with composites which are processed conventionally. Among the chief advantages of in-situ processing techniques, improved mechanical characteristics, the possibility of unique microstructure production, the simplicity of the process and cheap raw starting materials can be mentioned [11–20].

Because of a combination of properties like high hardness, high melting temperature, remarkable chemical stability, high strength, excellent abrasion resistance and high electrical and thermal conductivity, titanium diboride has been considered as a promising material for a wide range of applications [21–31]. Bio-coating on pure titanium, crucibles, cutting tools, cathodes and abrasion-resistance parts are among the most important applications of this fascinating ceramic [21,22,26,28–30]. Nevertheless, besides the inherent brittleness of purely sintered titanium diboride, the low sinterability is an obstacle toward the use of this material in some applications [32–40]. This poor sinterability comes back to the strong covalent bonding between titanium and bore atoms and the fairly low self-diffusion coefficient. In addition, the oxide layers covered the surface of TiB_2, namely B_2O_3 and TiO_2, implement a harmful effect on the consolidation process [27,28,41]. On the other hand, sintering at high temperatures leads to exaggerated grain growth and consequently lower fracture toughness [27,30,38].

Over a recent couple of decades, lots of efforts have been done to surmount these limitations. Investigation of the influence of sintering aid materials and also the development of new production techniques were among these admirable endeavors. In the term of additives, the effect of a wide range of ceramic aids, including carbon nanotubes (CNTs), SiC, AlN, Si_3N_4, $MoSi_2$, TiC, Al_2O_3, NbC, B_4C, WC, TiS_2, ZrB_2, TaC, TiN, etc., and metallic sintering aids, such as Cr, Co, Cu, Fe, Ni, Al, Ti, Ta, etc., on the mechanical properties and microstructure of TiB_2-based composites have been scrutinized [36,37,42–49]. Moreover, an advanced fabrication method named spark plasma sintering (SPS) has been developed to obtain finer grain ceramic materials at relatively lower temperatures compared with other conventional methods [50–64].

Several studies have been implemented on the fabrication parameters and role of additives on mechanical characteristics and

* Corresponding author.
E-mail address: shahedi@uma.ac.ir (M. Shahedi Asl).

https://doi.org/10.1016/j.ijrmhm.2019.02.022
Received 8 January 2019; Received in revised form 21 February 2019; Accepted 25 February 2019
Available online 26 February 2019

Table 1
Technical information of initial powders.

Material	Supplier	Particle Size (μm)	Purity (%)
TiB_2	China (Xuzhou Hongwu Co.)	3–8	99.9
SiC	China (Xuzhou Hongwu Co.)	< 0.5	99.0
TiN	China (Xuzhou Hongwu Co.)	1–3	99.5

microstructure of titanium diboride-based ceramics. Adding Si_3N_4 as a lonely sintering aid as well as Si_3N_4 and SiC at the same time on the improvement of the relative density of SPSed TiB_2 at the sintering circumstances of 1900 °C and 7 min dwell time were investigated and the figures of 99.7% and 99.9% were reported, respectively [65,66]. It was shown that use of TiC as a sintering aid led to a better fracture toughness because of achieving a finer microstructure [67]. The effect of sintering temperature on the grain growth was evaluated on monolithic TiB_2 and a comparison was done between the SPS technique and the conventional method on the mechanical properties of undoped titanium diboride [68,69]. AlN was added to TiB_2 to fabricate cutting tools and about 6.5 MPa $m^{1/2}$ fracture toughness and relative density of 92% was obtained when the sample sintered at 1800 °C by SPS technique [70,71]. Moreover, the use of Ti as a metallic sintering additive was examined and a fascinating combination of fine microstructure and mechanical properties (microhardness of ~27 GPa, fracture toughness of ~6 MPa $m^{1/2}$ and flexural strength of ~560 MPa and) were obtained by SPS technique at 1650 °C for 5 min under 50 MPa pressure [72].

In this research, the influences of TiN as an additive on the relative density and the microstructure of TiB_2-SiC system were evaluated. Two samples of TiB_2-SiC (20 vol%) and TiB_2-SiC (20 vol%)-TiN (5 wt%) were densified through the SPS method under the sintering conditions of 1900 °C, 7 min dwell time and 40 MPa external pressure. Study on the microstructure and chemical reactions over the sintering stage were done by SEM, EDS, XRD and thermodynamic evaluations using HSC software.

2. Experimental

2.1. Materials and process

As it is presented in Table 1, commercially available titanium diboride, as the matrix, and silicon carbide and titanium nitride as a reinforcement and a sintering aid, respectively, were used as initial powders, according to the information introduced by the suppliers. All powders were weighted to prepare two different mixture of powders, namely TiB_2-SiC (20 vol%) and TiB_2-SiC (20 vol%)-TiN (5 wt%) Then, the mixtures were dispersed in a WUC-D10H ultrasonic bath (Daihan, Korea) in ethanol for 0.5 h. The processes of heating and drying the prepared slurries were done using a MR 3001 K hot plate agitator (Heidolph, Germany) at the temperature of 120 °C for 3 h and a Universal Oven Um (Memmert, Germany) at 110 °C for one day, respectively. Afterward, the fully dried mixtures were crushed by a mill (both balls and cup fabricated of zirconia) and passed through a 100-mesh sieve. Fig. 1 shows the XRD spectra of prepared powder mixtures. Eventually, for producing the disk-shaped specimens (12 mm in radius and 5 mm in height), prepared mixtures were loaded into a die fabricated of graphite and sintered at the conditions of 1900 °C, 7 min holding time and 40 MPa pressure by an SPS machine (Nanozint 10i, Khala Poushan Felez Co., Iran) under the vacuum.

2.2. Characterization

The theoretical density was computed using the rule of mixtures and Archimedes' principles were applied for measuring the bulk density of produced composites. The relative density of as-produced ceramics was determined by the ratio calculation of the bulk and theoretical densities. Microstructural evaluations on the samples surfaces (both polished and fracture ones) of as-produced specimens were implemented via a Mira3 FESEM (Tescan, Czech Republic). For determination of grain size and check the accuracy of the figures obtained for the relative densities, an image analyzer software, namely ImageJ software ver. 1.52a (Wayne Rasband, USA), was used. In addition, the phase analysis of prepared composites was done using an XRD (Philips PW1730). For carrying out of the elemental analysis of as-sintered samples, an EDS (DXP-X10P) attached to SEM was used. Ultimately, HSC software (Outokumpu, Finland) was utilized for checking the possibility of chemical reactions occurred during the sintering stage.

3. Results and discussion

A relative density of 99.9 was obtained using a reinforcement of SiC to the TiB_2-based composite. In comparison with the monolithic TiB_2 spark plasma sintered at the same sintering circumstances [65] (relative density of 96.7%), adding SiC reinforcement led to a significant improvement in densification. Using TiN as a sintering aid also resulted in a fully dense composite (relative density of 99.9) at the same sintering conditions, showing TiN additive did not have a harmful effect on the densification. Fig. 2 shows the SEM images captured on the polished surfaces of sintered TiB_2-SiC (20 vol%) and TiB_2 –SiC (20 vol%)-TiN (5 wt%). Looking into these images, no porosity was detectable,

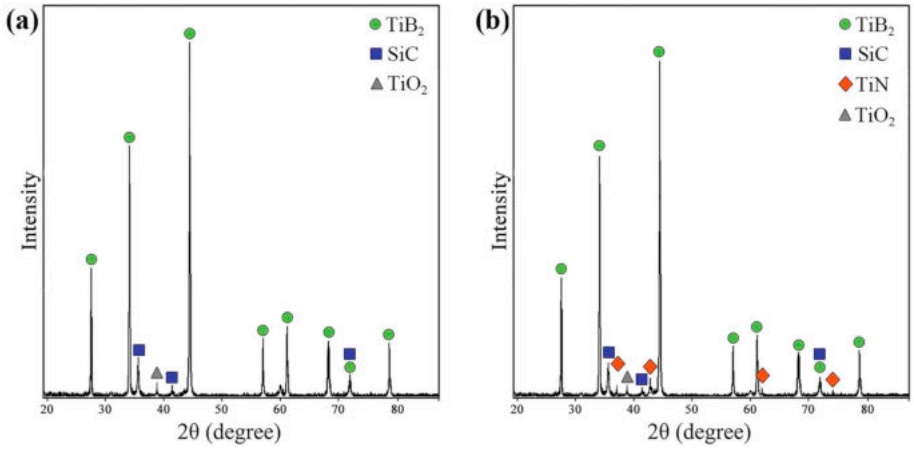

Fig. 1. XRD patterns of prepared powder mixtures (a) TiB_2-SiC and (b) TiB_2-SiC-TiN.

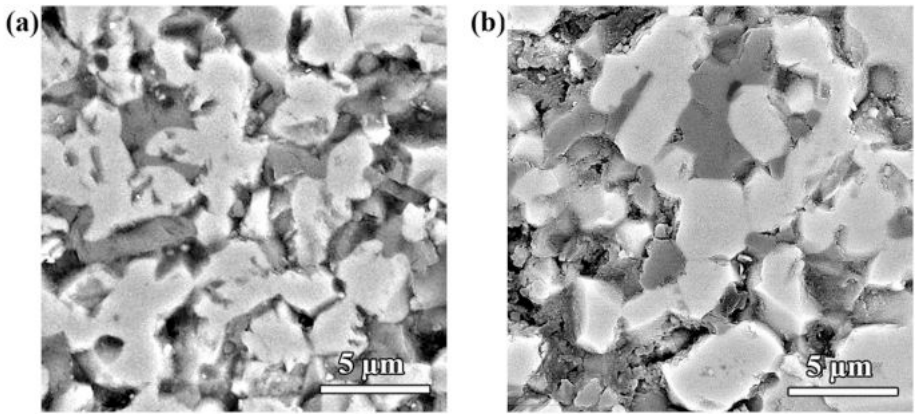

Fig. 2. SEM images (polished surfaces) of specimens sintered at 1900 °C (a) TiB_2-SiC (20 vol%) and (b) TiB_2-SiC (20 vol%)-TiN (5 wt%).

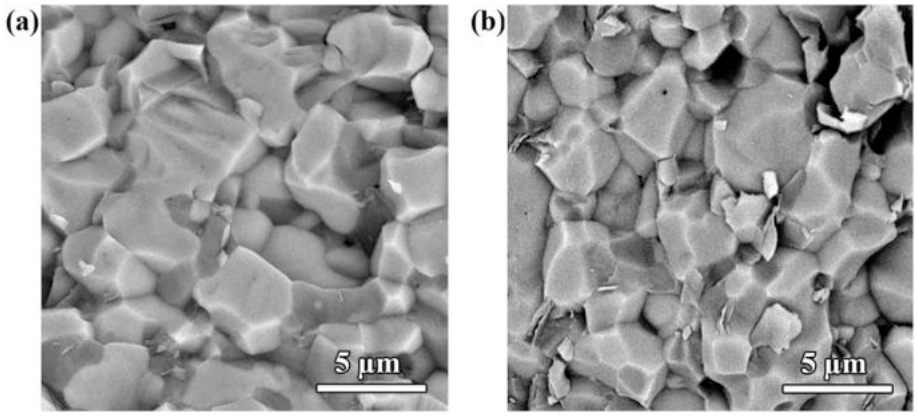

Fig. 3. SEM fractographs of specimens sintered at 1900 °C (a) TiB_2-SiC (20 vol%) and (b) TiB_2-SiC (20 vol%)-TiN (5 wt%).

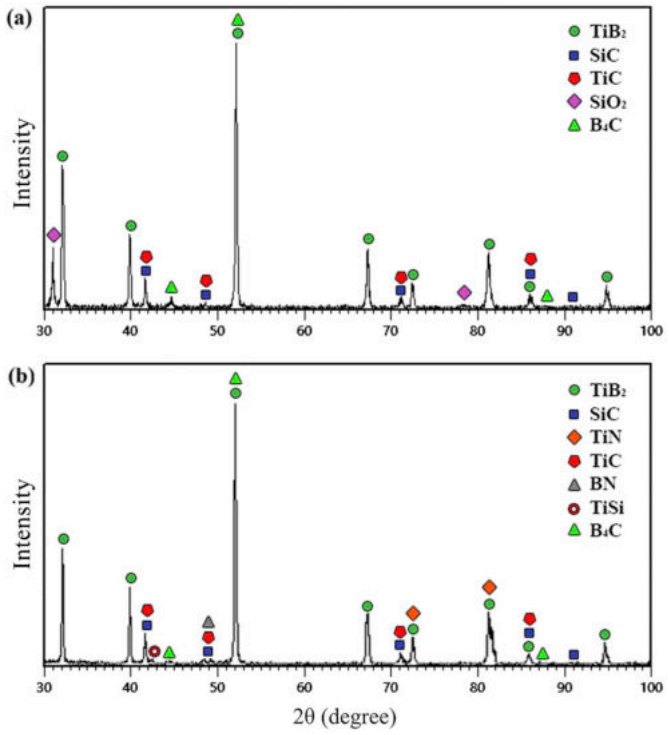

Fig. 4. XRD patterns of SPSed specimens (a) TiB_2-SiC (20 vol%) and (b) TiB_2-SiC (20 vol%)-TiN (5 wt%).

showing a complete densification stage. The black-colored regions which are observed in the micrographs are related to polishing artifacts including pulling out of hard grains and phases. As it is obvious, grains in both samples are utterly connected to each other, presenting the perfect sinterability of TiB_2 doped with 20 vol% SiC as a reinforcement, regardless using TiN as an additive.

Fig. 3 presents the SEM fractographs of TiN-free and TiN-doped TiB_2-SiC composite specimens. According to the size of initial TiB_2 powders (3–8 μm), it can be seen that no significant grain growth happened over the SPS process because of the size of most grains in both samples which are < 8 μm. The average grain size for the monolithic titanium diboride was reported 9.2 μm at the same sintering circumstances [65] which shows the beneficial influence of SiC reinforcement on the inhibition of grain growth in the TiB_2-based composite. As a result, it can be concluded that in addition of short dwell time which leads to a fine microstructure in SPS method, using SiC can obtain a finer microstructure and consequently better mechanical properties, thanks to the formation of several in-situ phases.

X-ray apparatus was utilized for phase characterizing of the TiB_2-SiC sample and the one doped with TiN additive. The patterns related to as-sintered composites are depicted in Fig. 4. According to Fig. 4a, crystalline phases of TiC, SiO_2 and B_4C as in-situ SPS products were identified in TiN-free sample, besides peaks related to TiB_2 and SiC as the initial materials. It should be noted that some part of detected SiO_2 in the XRD pattern (Fig. 4a) can be related to the presence of such oxide impurity on the surface of ultra-fine SiC particles as a starting material. Microstructural, phase and elemental characteristics of the as-purchased SiC powder are presented in Fig. 5. The SEM image, shown in Fig. 5a, verifies that the size of particles is submicron. Detection of some SiO_2 peaks in the XRD spectrum (Fig. 5b) and oxygen element in the

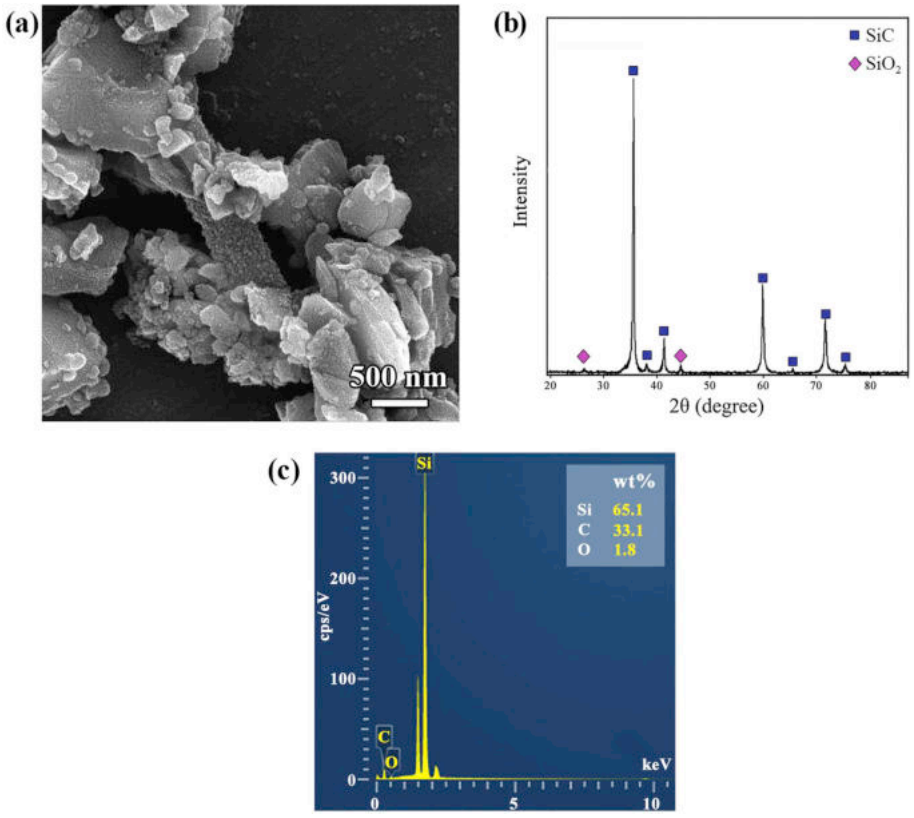

Fig. 5. (a) SEM image, (b) XRD pattern and (c) EDS spectrum of as-received SiC powder.

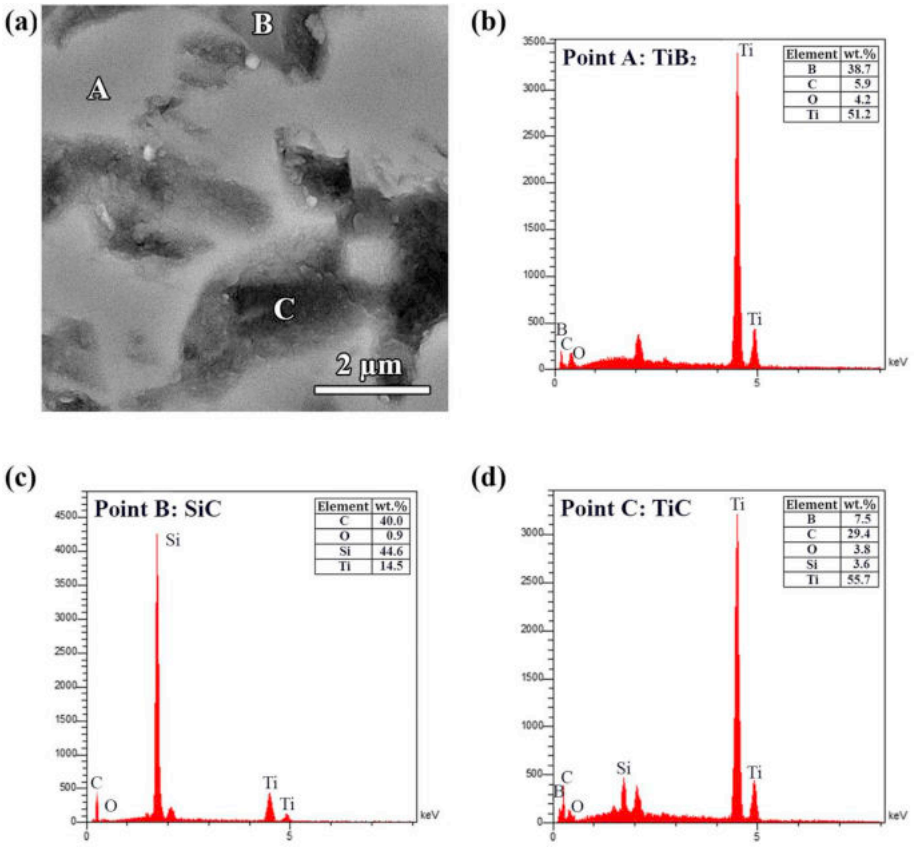

Fig. 6. SEM micrograph of the polished surface of TiB_2-SiC (20 vol%) and related EDS results.

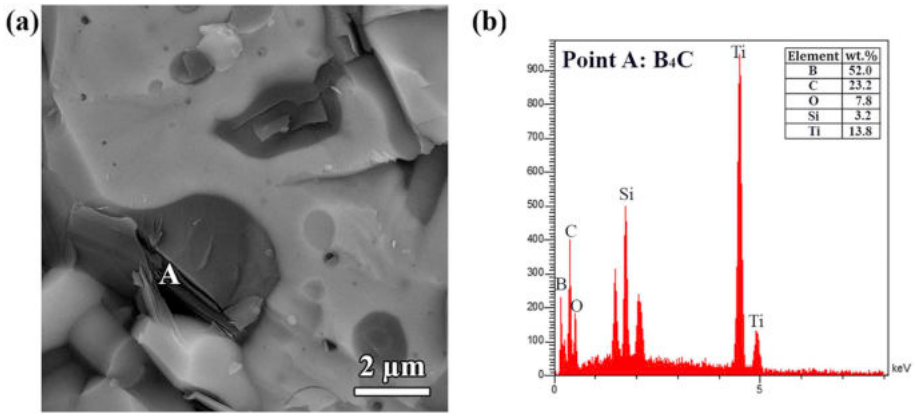

Fig. 7. SEM micrograph of the fracture surface of TiB_2-SiC (20 vol%) and related EDS result.

EDS spectrum (Fig. 5c) verifies the presence of SiO_2 in the starting material. Germi et al. [66] reported the formation of TiO_2 and B_2O_3 oxide layer on the surface of initial titanium diboride powders. Moreover, the sintering process led to decrease the oxygen level in the final product due to the chemical reactions among starting combinations. The feasibility of the reaction between the TiO_2 oxide layer and SiC which can result to TiC and SiO_2 products was investigated by HSC chemical software (Eq. (1)). ΔG of this reaction is −80 kJ, indicating favorability of it in the term of thermodynamics. The in-situ formation of SiO_2 and TiC phases, which are visible in the XRD pattern shown in Fig. 4a, proves the validity of the reaction.

$$SiC + TiO_2 = SiO_2 + TiC \quad (1)$$

In addition, the formation of SiO_2 during the sintering process can lead to densification improvement in the as-sintered composite through the liquid phase sintering mechanism. The oxide layer of B_2O_3 melts and boils at the temperatures of 450 °C and 1860 °C in the standard condition of 1 atm, respectively. Thanks to the level of vacuum of the sintering environment, evaporation of B_2O_3 takes place at the temperatures below 1600 °C. Eventually, the B_2O_3 vapor reacts with SiC, based on Eq. (2), producing B_4C and some other byproducts in the gaseous phase. In the term of thermodynamics, the reaction mentioned in Eq. (2) is favorable at the temperatures higher than 1750 °C. Looking into the XRD pattern in Fig. 4a, B_4C formation over the sintering process is clear and other gaseous phases can evacuate because of the vacuum circumstances into the sintering chamber [66].

$$4B_2O_3\,(g) + 7SiC = 2B_4C + 7SiO\,(g) + 5CO\,(g) \quad (2)$$

Fig. 4b illustrates XRD pattern when 5 wt% TiN was added to the composite sample. As it is obvious, adding both TiN and SiC at the same time to TiB_2 was resulted in the formation of B_4C, TiSi, BN and TiC, but SiO_2 phase seen in the TiN-free sample was not detectable in the TiN-doped sample. TiC phase, as it was discussed before, can produce base on the Eq. (1): the product of interaction between SiC and TiO_2 phases during spark plasma sintering process. According to Eqs. (3)–(4), adding TiN as a sintering aid to the TiB_2-SiC composite, has led to some other reactions resulted to consume all SiO_2 content formed with TiC based on Eq. (1). According to Eqs. (3)–(4), the reaction of SiO_2 with TiO_2 and TiN can result in the formation of TiSi and Si_3N_4 and some other gaseous products, respectively. These two reactions are favorable at ultrahigh temperatures (> 5205 °C and 3396 °C, respectively) in the standard conditions. Due to the application of high pressure during the SPS process and also the possibility of locally reaching to such ultrahigh temperatures under the SPS process, progressing of Eqs. (3)–(4) are utterly possible. The formation of TiSi phase was already proved by the XRD investigation.

$$SiO_2 + TiO_2 = TiSi + 2O_2\,(g) \quad (3)$$

$$3SiO_2 + 6\,TiN = Si_3N_4 + 6\,TiO\,(g) + N_2\,(g) \quad (4)$$

In addition, TiB_2 and TiN can react with each other under certain circumstances. According to Eqs. (5)–(7), when these two phases would place in close vicinity under the high temperature condition, titanium nitride loses N and titanium boride loses B, and consequently, the formation of hBN would be possible [73].

$$TiN = TiN_{1-a} + a\,(1/2)\,N_2 \quad (5)$$

$$TiB_2 = TiB_{2-b} + bB \quad (6)$$

$$\Delta\,(1/2)\,N_2 + \Delta B = \Delta BN\,(\Delta = \min(a, b)) \quad (7)$$

Fig. 6 shows a magnified view of the composite of TiB_2 modified by SiC captured by SEM. As it is clear, three different phases are visible in this image. The EDS results of these phases are also presented in Fig. 6. The bright area labeled by A letter is related to the TiB_2 matrix with a high concentration of Ti and B elements. Two other areas labeled by B and C are contributed to SiC and in-situ TiC phase which are rich in Si/C and Ti/C as major elements, respectively. Fig. 7 also presents a close view of the fracture surface of TiB_2-SiC ceramic, captured by SEM, showing the in-situ formed B_4C phase over the SPS process.

As it was discussed before, adding TiN to the TiB_2-SiC system led to the formation of various new phases over the SPS process, including TiC, BN, TiSi and B_4C. Fig. 8 indicates SEM micrograph of the polished surface of TiB_2-SiC-TiN composite. The related EDS results of different regions are also shown in Fig. 8 for a better estimation of the microstructure. The area labeled by A letter which is rich in Ti and B elements is attributed to the TiB_2 matrix. The small region surrounded by titanium diboride matrix, shown by B letter, may be associated with in-situ formed TiSi phase due to the elemental analysis. The area rich in Si and C, labeled with C letter, is related to the unreacted SiC initial phase. Finally, point D presented an area with a high concentration of Ti, C and B elements which may be representative of TiC and B_4C phases formed in-situ. Fig. 9 shows SEM fractograph of TiN-doped composite and the associated EDS spectra, indicating the formation of hBN nanoplatelets in this sample. Unfortunately, other secondary formed phases could not be found in SEM micrographs because of their negligible contents.

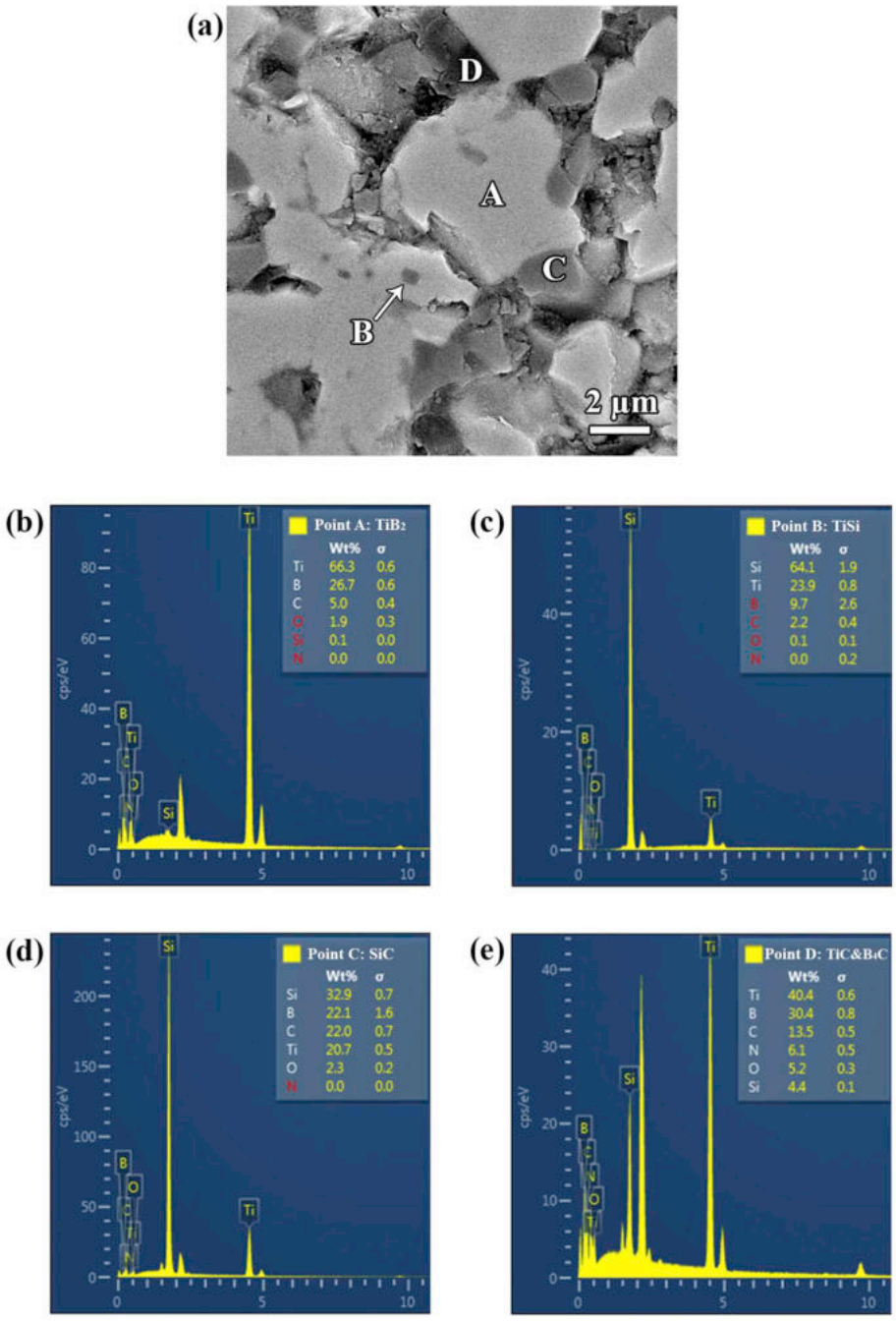

Fig. 8. SEM micrograph of the polished surface of TiB_2-SiC (20 vol%)-TiN (5 wt%) and related EDS results.

4. Conclusions

The influences of adding SiC as a reinforcement and TiN as a sintering additive was examined on the relative density, microstructure and formation of in-situ phases in TiB_2-based composites. Two different samples of TiB_2-SiC and TiB_2-SiC-TiN were sintered using a SPS technique and sintering conditions of 1900 °C, 7 min dwell time and 40 MPa pressure. After the SPS process, both specimens reached their theoretical densities. Various in-situ phases were formed in each composite: TiC, SiO_2 and B_4C in TiN-free sample and TiC, BN, TiSi and B_4C in the doped one. The presence/formation of SiO_2 phase had a positive role during the sintering process: as a liquid phase in the TiN-free ceramic leading to a better sinterability and as a reactant for forming in-situ TiSi phase in the TiB_2-SiC-TiN composite.

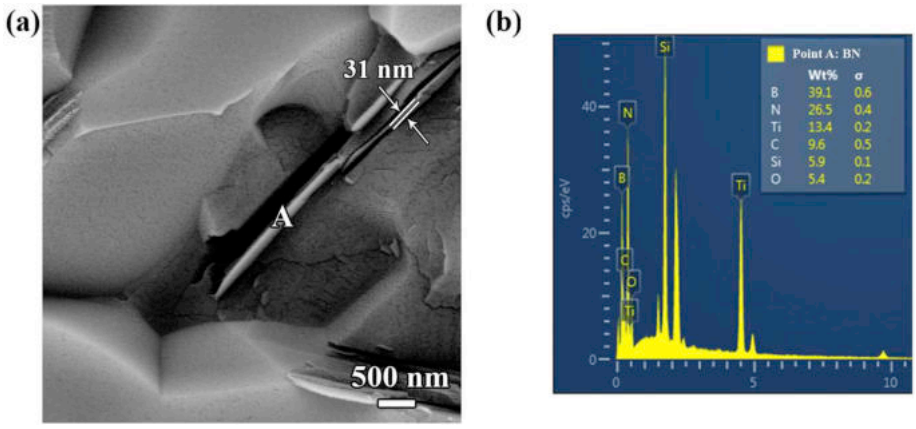

Fig. 9. SEM micrograph of the fracture surface of TiB_2-SiC (20 vol%)-TiN (5 wt%) and related EDS result.

References

[1] Z. Ahmadi, B. Nayebi, M. Shahedi Asl, M. Ghassemi Kakroudi, Fractographical characterization of hot pressed and pressureless sintered AlN-doped ZrB2–SiC composites, Mater. Charact. 110 (Dec. 2015) 77–85.

[2] Z. Ahmadi, B. Nayebi, M. Shahedi Asl, M. Ghassemi Kakroudi, I. Farahbakhsh, Sintering behavior of ZrB2–SiC composites doped with Si3N4: a fractographical approach, Ceram. Int. 43 (13) (Sep. 2017) 9699–9708.

[3] M. Shahedi Asl, B. Nayebi, Z. Ahmadi, M. Jaberi Zamharir, M. Shokouhimehr, Effects of carbon additives on the properties of ZrB2–based composites: a review, Ceram. Int. 44 (7) (May 2018) 7334–7348.

[4] D.C. Ferreira, E. dos Magalhães, R.F. Brito, E. Silva, Numerical analysis of the influence of coatings on a cutting tool using COMSOL, Int. J. Adv. Manuf. Technol. 97 (1–4) (Jul. 2018) 1305–1314.

[5] Z. Degui, et al., In-situ HIP synthesis of TiB2/SiC ceramic composites, J. Mater. Process. Technol. 89–90 (May 1999) 457–461.

[6] J. Song, C. Huang, B. Zou, H. Liu, J. Wang, Microstructure and mechanical properties of TiB2–TiC–WC composite ceramic tool materials, Mater. Des. 36 (Apr. 2012) 69–74.

[7] M. Shahedi Asl, M.J. Zamharir, Z. Ahmadi, S. Parvizi, Effects of nano-graphite content on the characteristics of spark plasma sintered ZrB2–SiC composites, Mater. Sci. Eng. A 716 (Feb. 2018) 99–106.

[8] M. Akhlaghi, S.A. Tayebifard, E. Salahi, M. Shahedi Asl, G. Schmidt, Self-propagating high-temperature synthesis of Ti3AlC2 MAX phase from mechanically-activated Ti/Al/graphite powder mixture, Ceram. Int. 44 (8) (2018) 9671–9678.

[9] I. Farahbakhsh, Z. Ahmadi, M. Shahedi Asl, Densification, microstructure and mechanical properties of hot pressed ZrB2–SiC ceramic doped with nano-sized carbon black, Ceram. Int. 43 (11) (Aug. 2017) 8411–8417.

[10] M. Shahedi Asl, I. Farahbakhsh, B. Nayebi, Characteristics of multi-walled carbon nanotube toughened ZrB2–SiC ceramic composite prepared by hot pressing, Ceram. Int. 42 (1) (Jan. 2016) 1950–1958.

[11] N. Pourmohammadie Vafa, M. Shahedi Asl, M. Jaberi Zamharir, M. Ghassemi Kakroudi, Reactive hot pressing of ZrB2-based composites with changes in ZrO2/SiC ratio and sintering conditions. Part I: densification behavior, Ceram. Int. 41 (7) (Aug. 2015) 8388–8396.

[12] N. Pourmohammadie Vafa, B. Nayebi, M. Shahedi Asl, M. Jaberi Zamharir, M. Ghassemi Kakroudi, Reactive hot pressing of ZrB2-based composites with changes in ZrO2/SiC ratio and sintering conditions. Part II: mechanical behavior, Ceram. Int. 42 (2) (Feb. 2016) 2724–2733.

[13] M. Shahedi Asl, Microstructure, hardness and fracture toughness of spark plasma sintered ZrB2–SiC–Cf composites, Ceram. Int. 43 (17) (Dec. 2017) 15047–15052.

[14] M. Shahedi Asl, A. Sabahi Namini, A. Motallebzadeh, M. Azadbeh, Effects of sintering temperature on microstructure and mechanical properties of spark plasma sintered titanium, Mater. Chem. Phys. 203 (Jan. 2018) 266–273.

[15] G.J. Zhang, X.M. Yue, Z.Z. Jin, Preparation and microstructure of TiB2-TiC-SiC platelet-reinforced ceramics by reactive hot-pressing, J. Eur. Ceram. Soc. 16 (10) (Jan. 1996) 1145–1148.

[16] L. Klinger, I. Gotman, D. Horvitz, In situ processing of TiB2/TiC ceramic composites by thermal explosion under pressure: experimental study and modeling, Mater. Sci. Eng. A 302 (1) (Apr. 2001) 92–99.

[17] Z. Balak, M. Azizieh, H. Kafashan, M. Shahedi Asl, Z. Ahmadi, Optimization of effective parameters on thermal shock resistance of ZrB2-SiC-based composites prepared by SPS: using Taguchi design, Mater. Chem. Phys. 196 (Aug. 2017) 333–340.

[18] Z. Balak, M. Shahedi Asl, M. Azizieh, H. Kafashan, R. Hayati, Effect of different additives and open porosity on fracture toughness of ZrB2–SiC-based composites prepared by SPS, Ceram. Int. 43 (2) (Feb. 2017) 2209–2220.

[19] B. Nayebi, M. Shahedi Asl, M. Ghassemi Kakroudi, I. Farahbakhsh, M. Shokouhimehr, Interfacial phenomena and formation of nano-particles in porous ZrB2–40 vol% B4C UHTC, Ceram. Int. 42 (15) (Nov. 2016) 17009–17015.

[20] M. Shahedi Asl, M. Ghassemi Kakroudi, F. Golestani-Fard, H. Nasiri, A Taguchi approach to the influence of hot pressing parameters and SiC content on the sinterability of ZrB2-based composites, Int. J. Refract. Met. Hard Mater. 51 (Jul. 2015) 81–90.

[21] A. Ebrahimi, H. Esfahani, A. Fattah-alhosseini, O. Imantalab, In-vitro electrochemical study of TiB/TiB2 composite coating on titanium in Ringer's solution, J. Alloys Compd. 765 (Oct. 2018) 826–834.

[22] J.Y. Dai, D.X. Li, H.Q. Ye, G.J. Zhang, Z.Z. Jin, Characterization of TiB2–Ti(CN)–Ni ceramics by transmission and analytical electron microscopy, Mater. Lett. 16 (6) (Jun. 1993) 317–321.

[23] Ö. Balcı, D. Ağaoğulları, H. Gökçe, İ. Duman, M.L. Öveçoğlu, Influence of TiB2 particle size on the microstructure and properties of Al matrix composites prepared via mechanical alloying and pressureless sintering, J. Alloys Compd. 586 (Feb. 2014) S78–S84.

[24] S.K. Bhaumik, C. Divakar, L. Rangaraj, A.K. Singh, Reaction sintering of NiAl and TiB2–NiAl composites under pressure, Mater. Sci. Eng. A 257 (2) (Dec. 1998) 341–348.

[25] P. Wyzga, L. Jaworska, M.M. Bucko, J. Bonarski, P. Putyra, P. Figiel, TiN–TiB2 composites prepared by various sintering techniques, Int. J. Refract. Met. Hard Mater. 41 (Nov. 2013) 571–576.

[26] A. Rabiezadeh, A.M. Hadian, A. Ataie, Synthesis and sintering of TiB2 nanoparticles, Ceram. Int. 40 (10) (Dec. 2014) 15775–15782.

[27] G. Zhao, C. Huang, H. Liu, B. Zou, H. Zhu, J. Wang, Microstructure and mechanical properties of TiB2–SiC ceramic composites by reactive hot pressing, Int. J. Refract. Met. Hard Mater. 42 (Jan. 2014) 36–41.

[28] W. Ji, et al., Fabrication and properties of TiB2-based cermets by spark plasma sintering with CoCrFeNiTiAl high-entropy alloy as sintering aid, J. Eur. Ceram. Soc. 35 (3) (Mar. 2015) 879–886.

[29] M. Kitiwan, A. Ito, J. Zhang, T. Goto, Densification and mechanical properties of cBN–TiN–TiB2 composites prepared by spark plasma sintering of SiO2-coated cBN powder, J. Eur. Ceram. Soc. 34 (15) (Dec. 2014) 3619–3626.

[30] A. Rabiezadeh, A. Ataie, A.M. Hadian, Sintering of Al2O3–TiB2 nano-composite derived from milling assisted sol–gel method, Int. J. Refract. Met. Hard Mater. 33 (Jul. 2012) 58–64.

[31] M. Vajdi, F. Sadegh Moghanlou, Z. Ahmadi, A. Motallebzadeh, M. Shahedi Asl, Thermal diffusivity and microstructure of spark plasma sintered TiB2-SiC-Ti composite, Ceram. Int. (Jan. 2019), https://doi.org/10.1016/j.ceramint.2019.01.141.

[32] M. Shahedi Asl, A. Sabahi Namini, M. Ghassemi Kakroudi, Influence of silicon carbide addition on the microstructural development of hot pressed zirconium and titanium diborides, Ceram. Int. 42 (4) (Mar. 2016) 5375–5381.

[33] A. Sabahi Namini, S.N. Seyed Gogani, M. Shahedi Asl, K. Farhadi, M. Ghassemi Kakroudi, A. Mohammadzadeh, Microstructural development and mechanical properties of hot pressed SiC reinforced TiB2 based composite, Int. J. Refract. Met. Hard Mater. 51 (Jul. 2015) 169–179.

[34] K. Farhadi, A. Sabahi Namini, M. Shahedi Asl, A. Mohammadzadeh, M. Ghassemi Kakroudi, Characterization of hot pressed SiC whisker reinforced TiB2 based composites, Int. J. Refract. Met. Hard Mater. 61 (Dec. 2016) 84–90.

[35] M. Shahedi Asl, Z. Ahmadi, S. Parvizi, Z. Balak, I. Farahbakhsh, Contribution of SiC particle size and spark plasma sintering conditions on grain growth and hardness of TiB2 composites, Ceram. Int. 43 (16) (Nov. 2017) 13924–13931.

[36] B. Basu, J. Vleugels, O. Van Der Biest, Fretting wear behavior of TiB2-based materials against bearing steel under water and oil lubrication, Wear 250 (1–12) (Oct. 2001) 631–641.

[37] J. Lin, Y. Yang, H. Zhang, Q. Lin, B. Zhu, Synthesis and characterization of in-situ CNTs reinforced TiB2-based composite by CVD using Ni catalysts, Ceram. Int. 44 (2) (Feb. 2018) 2042–2047.

[38] M. Shahedi Asl, M. Ghassemi Kakroudi, A processing-microstructure correlation in ZrB2–SiC composites hot-pressed under a load of 10 MPa, Univ. J. Mater. Sci. 3 (1) (2015) 14–21.

[39] M. Shahedi Asl, M. Ghassemi Kakroudi, B. Nayebi, A fractographical approach to the sintering process in porous ZrB2–B4C binary composites, Ceram. Int. 41 (1) (Jan. 2015) 379–387.

[40] M. Shahedi Asl, M. Ghassemi Kakroudi, Fractographical assessment of densification mechanisms in hot pressed ZrB2-SiC composites, Ceram. Int. 40 (9) (Nov. 2014) 15273–15281.
[41] Z. Ahmadi, B. Nayebi, M. Shahedi Asl, I. Farahbakhsh, Z. Balak, Densification improvement of spark plasma sintered TiB2-based composites with micron-, submicron- and nano-sized SiC particulates, Ceram. Int. 44 (10) (Jul. 2018) 11431–11437.
[42] T.S.R.C. Murthy, R. Balasubramaniam, B. Basu, A.K. Suri, M.N. Mungole, Oxidation of monolithic TiB2 and TiB2–20wt.% MoSi2 composite at 850°C, J. Eur. Ceram. Soc. 26 (1–2) (Jan. 2006) 187–192.
[43] K. Cymerman, D. Oleszak, M. Rosinski, A. Michalski, Structure and mechanical properties of TiB2/TiC–Ni composites fabricated by pulse plasma sintering method, Adv. Powder Technol. 29 (8) (Aug. 2018) 1795–1803.
[44] D. Demirskyi, H. Borodianska, Y. Sakka, O. Vasylkiv, Ultra-high elevated temperature strength of TiB2-based ceramics consolidated by spark plasma sintering, J. Eur. Ceram. Soc. 37 (1) (Jan. 2017) 393–397.
[45] L. Nikzad, R. Licheri, T. Ebadzadeh, R. Orrù, G. Cao, Effect of ball milling on reactive spark plasma sintering of B4C–TiB2 composites, Ceram. Int. 38 (8) (Dec. 2012) 6469–6480.
[46] Z. Fu, R. Koc, Pressureless sintering of TiB2 with low concentration of Co binder to achieve enhanced mechanical properties, Mater. Sci. Eng. A 721 (Apr. 2018) 22–27.
[47] N. Wu, F. Xue, Q. Yang, H. Yang, J. Ruan, Microstructure and mechanical properties of TiB2-based composites with high volume fraction of Fe-Ni additives prepared by vacuum pressureless sintering, Ceram. Int. 43 (1) (Jan. 2017) 1394–1401.
[48] G. Zhao, C. Huang, H. Liu, B. Zou, H. Zhu, J. Wang, A study on in-situ synthesis of TiB2–SiC ceramic composites by reactive hot pressing, Ceram. Int. 40 (1) (Jan. 2014) 2305–2313.
[49] S. Tuffé, J. Dubois, G. Fantozzi, G. Barbier, Densification, microstructure and mechanical properties of TiB2-B4C based composites, Int. J. Refract. Met. Hard Mater. 14 (5–6) (Jan. 1996) 305–310.
[50] A. Sabahi Namini, M. Azadbeh, M. Shahedi Asl, Effect of TiB2 content on the characteristics of spark plasma sintered Ti–TiBw composites, Adv. Powder Technol. 28 (6) (Jun. 2017) 1564–1572.
[51] M. Shahedi Asl, A statistical approach towards processing optimization of ZrB2–SiC–graphite nanocomposites. Part I: relative density, Ceram. Int. 44 (6) (Apr. 2018) 6935–6939.
[52] Y. Azizian-Kalandaragh, A.S. Namini, Z. Ahmadi, M. Shahedi Asl, Reinforcing effects of SiC whiskers and carbon nanoparticles in spark plasma sintered ZrB2 matrix composites, Ceram. Int. 44 (16) (Nov. 2018) 19932–19938.
[53] E. Ghasali, M. Shahedi Asl, Microstructural development during spark plasma sintering of ZrB2–SiC–Ti composite, Ceram. Int. 44 (15) (Oct. 2018) 18078–18083.
[54] M. Shahedi Asl, B. Nayebi, Z. Ahmadi, S. Parvizi, M. Shokouhimehr, A novel ZrB2–VB2–ZrC composite fabricated by reactive spark plasma sintering, Mater. Sci. Eng. A 731 (Jul. 2018) 131–139.
[55] M. Shahedi Asl, B. Nayebi, M. Shokouhimehr, TEM characterization of spark plasma sintered ZrB2–SiC–graphene nanocomposite, Ceram. Int. 44 (13) (Sep. 2018) 15269–15273.
[56] A. Babapoor, M.S. Asl, Z. Ahmadi, A.S. Namini, Effects of spark plasma sintering temperature on densification, hardness and thermal conductivity of titanium carbide, Ceram. Int. 44 (12) (Aug. 2018) 14541–14546.
[57] A. Sabahi Namini, Z. Ahmadi, A. Babapoor, M. Shokouhimehr, M. Shahedi Asl, Microstructure and thermomechanical characteristics of spark plasma sintered TiC ceramics doped with nano-sized WC, Ceram. Int. 45 (2) (Feb. 2019) 2153–2160.
[58] M. Akhlaghi, S.A. Tayebifard, E. Salahi, M. Shahedi Asl, Spark plasma sintering of TiAl–Ti3AlC2 composite, Ceram. Int. 44 (17) (Dec. 2018) 21759–21764.
[59] S.A. Delbari, B. Nayebi, E. Ghasali, M. Shokouhimehr, M. Shahedi Asl, Spark plasma sintering of TiN ceramics codoped with SiC and CNT, Ceram. Int. 45 (3) (Feb. 2019) 3207–3216.
[60] A. Sabahi Namini, A. Motallebzadeh, B. Nayebi, M. Shahedi Asl, M. Azadbeh, Microstructure–mechanical properties correlation in spark plasma sintered Ti–4.8 wt.% TiB2 composites, Mater. Chem. Phys. 223 (Feb. 2019) 789–796.
[61] B. Mohammadpour, Z. Ahmadi, M. Shokouhimehr, M. Shahedi Asl, Spark plasma sintering of Al-doped ZrB2–SiC composite, Ceram. Int. 45 (4) (Mar. 2019) 4262–4267.
[62] G. CAO, H. Xu, Z. Zheng, L. Geng, N. Masaaki, Grain size effect on cyclic oxidation of (TiB2 + TiC)/Ni3Al composites, Trans. Nonferrous Met. Soc. China 22 (7) (Jul. 2012) 1588–1593.
[63] S. Parvizi, Z. Ahmadi, M.J. Zamharir, M. Shahedi Asl, Synergistic effects of graphite nano-flakes and submicron SiC particles on the characteristics of spark plasma sintered ZrB2 nanocomposites, Int. J. Refract. Met. Hard Mater. 75 (Sep. 2018) 10–17.
[64] A. Sabahi Namini, M. Azadbeh, M. Shahedi Asl, Effects of in-situ formed TiB whiskers on microstructure and mechanical properties of spark plasma sintered Ti–B4C and Ti–TiB2 composites, Sci. Iran 25 (2) (Sep. 2018) 762–771.
[65] Z. Hamidzadeh Mahaseni, M. Dashti Germi, Z. Ahmadi, M. Shahedi Asl, Microstructural investigation of spark plasma sintered TiB2 ceramics with Si3N4 addition, Ceram. Int. 44 (11) (Aug. 2018) 13367–13372.
[66] M. Dashti Germi, Z. Hamidzadeh Mahaseni, Z. Ahmadi, M. Shahedi Asl, Phase evolution during spark plasma sintering of novel Si3N4-doped TiB2–SiC composite, Mater. Charact. 145 (Nov. 2018) 225–232.
[67] S.K. Bhaumik, C. Divakar, A.K. Singh, G.S. Upadhyaya, Synthesis and sintering of TiB2 and TiB2–TiC composite under high pressure, Mater. Sci. Eng. A 279 (1–2) (Feb. 2000) 275–281.
[68] Ö. Balcı, U. Burkhardt, M. Schmidt, J. Hennicke, M. Barış Yağcı, M. Somer, Densification, microstructure and properties of TiB2 ceramics fabricated by spark plasma sintering, Mater. Charact. 145 (Nov. 2018) 435–443.
[69] W. Wang, Z. Fu, H. Wang, R. Yuan, Influence of hot pressing sintering temperature and time on microstructure and mechanical properties of TiB2 ceramics, J. Eur. Ceram. Soc. 22 (7) (Jul. 2002) 1045–1049.
[70] L.A.F. Peçanha, et al., Characterization of TiB2-AlN composites for application as cutting tool, J. Mater. Res. Technol. 7 (4) (Oct. 2018) 550–553.
[71] L.A.F. Júnior, Í.V. Tomaz, M.P. Oliveira, L. Simão, S.N. Monteiro, Development and evaluation of TiB2–AlN ceramic composites sintered by spark plasma, Ceram. Int. 42 (16) (Dec. 2016) 18718–18723.
[72] Z.-H. Zhang, X.-B. Shen, F.-C. Wang, S.-K. Lee, Q.-B. Fan, M.-S. Cao, Low-temperature densification of TiB2 ceramic by the spark plasma sintering process with Ti as a sintering aid, Scr. Mater. 66 (3–4) (Feb. 2012) 167–170.
[73] F. Shayesteh, S.A. Delbari, Z. Ahmadi, M. Shokouhimehr, M. Shahedi Asl, Influence of TiN dopant on microstructure of TiB2 ceramic sintered by spark plasma, Ceram. Int. 45 (5) (Nov. 2019) 5306–5311.